

## Comparative Study of Pyridine and Pyrimidine Derivatives as Corrosion Inhibitors of C38 Steel in Molar HCl

A. Ghazoui<sup>1</sup>, R. Saddik<sup>1</sup>, N. Benchat<sup>1</sup>, M. Guenbour<sup>2</sup>, B. Hammouti<sup>1,3,\*</sup>, S.S. Al-Deyab<sup>3</sup>, A. Zarrouk<sup>1</sup>

<sup>1</sup> LCAE-URAC18, Faculte des Sciences, Universite Mohammed Premier B.P. 717, 60000 Oujda, Morocco.

<sup>2</sup> Laboratoire d'Electrochimie, Corrosion et Environnement, Faculte des Sciences, Rabat – Morocco.

<sup>3</sup> Petrochemical Research Chair, Chemistry Department, College of Science, King Saud University, P.O. Box 2455, Riyadh 11451, Saudi Arabia

\*E-mail: [hammoutib@gmail.com](mailto:hammoutib@gmail.com)

Received: 24 June 2012 / Accepted: 13 July 2012 / Published: 1 August 2012

---

Corrosion inhibition of C38 steel in 1 M HCl was investigated in the absence and presence of different concentrations of two imidazo derivatives namely, 2-phenylimidazo[1,2-a]pyridine (P1) and 2-(*m*-methoxyphenyl) imidazo[1,2-a]pyrimidine (P5). Weight loss, potentiodynamic polarization and electrochemical impedance spectroscopy techniques were employed. Impedance measurements showed that the double-layer capacitance decreased and charge-transfer resistance increased with increase in the inhibitors concentration and hence increasing in inhibition efficiency. Potentiodynamic polarization study showed that all the inhibitors act as mixed-type inhibitors. The inhibitors were adsorbed on the steel surface according to the Langmuir adsorption isotherm model. From the adsorption isotherm, some thermodynamic data for the adsorption process were calculated and discussed. Kinetic parameters activation such as activation energy, pre-exponential factor, enthalpy of activation and entropy of activation were evaluated from the effect of temperature on corrosion and inhibition processes.  $E$  (%) values obtained from various methods used are in good agreement.

---

**Keywords:** Corrosion; Imidazopyridine derivatives; HCl; C38 steel; Potentiodynamic polarisation; EIS.

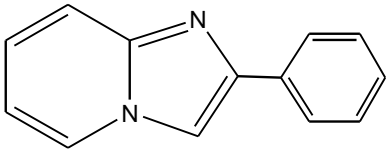
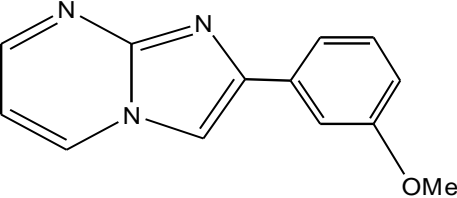
### 1. INTRODUCTION

Hydrochloric acid solutions are widely used in chemical and several industrial processes such as acid pickling, acid cleaning, acid descaling and oil well acidizing, which require the use of corrosion inhibitors [1-5].

*N*-heterocyclic compounds are well qualified to play more protection for steel corrosion [6-8]. Many *N*-heterocyclic compounds such as derivatives of pyrazole [9-11], bipyrazole [12-14],

triazole [15-17], tetrazole [18-20], imidazole [21-24], pyridine [25-28], pyrimidine [29], pyridazine [30,31] and imidazopyridine [32] have been reported as effective corrosion inhibitors for steel in acidic media. The heterocyclic compound containing nitrogen atoms can easily be protonated in acidic medium to exhibit good inhibitory action on the corrosion of metals in acid solutions.

The present study aimed to test new compounds named 2-phenylimidazo[1,2-a]pyridine (P1) and 2-(m-methoxyphenyl) imidazo[1,2-a]pyrimidine (P5) on the corrosion of mild steel in 1.0 M hydrochloric acid solution. The study has been evaluated using weight loss, potentiodynamic polarization and EIS techniques at various concentrations ( $1 \times 10^{-6} \text{M} - 1 \times 10^{-3} \text{M}$ ) of P1 and P5. The study also aimed to show the influence of addition of nitrogen atom in the pyridine ring to obtain pyrimidine one. The chemical structures of the studied imidazo-pyridine derivatives are given in Figure 1.

Name	Chemical Structure	Abbreviation
2-phenylimidazo[1,2-a]pyridine		P <sub>1</sub>
2-(m-methoxyphenyl) imidazo[1,2-a]pyrimidine		P <sub>5</sub>

**Figure 1.** The molecular structure of the studied imidazo-pyridine derivatives.

## 2. EXPERIMENTAL DETAILS

### 2.1. Materials and reagents

C38 Steel strips containing (0.09 % P; 0.38 % Si; 0.01 % Al; 0.05 % Mn; 0.21 % C; 0.05 % S and the remainder iron) were used for electrochemical and gravimetric studies. Prior to all measurements, are abraded with a series of emery paper up to 1200 grade. The specimens are washed thoroughly with bidistilled water degreased and dried with acetone. The aggressive solution (1M HCl) was prepared by dilution of Analytical Grade 35.4 % HCl with double-distilled water.

### 2.2. Synthesis

#### P1

The 2-phenyl imidazo[1,2-a]pyridine (P1) was provides by *Benchat* and co-workers, by the following method [34]. The synthetic strategy involves condensation of 2-amino pyridine with (37.64

g, 0.4 mole) bromoacetophenone (48.75 g, 0.25 mole) in boiling ethanol for five hours, after cooling the solution the mixture has neutralized at 0° C with Na<sub>2</sub>CO<sub>2</sub>, the products are extracted with dichloromethane. The organic layer is dried over sodium sulphate and the dichloromethane is removed under reduced pressure. The crude products are purified on a silica gel column and a colourless solid is obtained. The 2-phenyl imidazo [1, 2-a]pyridine compound is obtained with a good yield 70 %.

White powder, M. p. = 139-141 °C;

RMN <sup>1</sup>H (300.134 MHz, CDCl<sub>3</sub>) δ(ppm): 7.90 (m, 3H, H<sub>5</sub>, H<sub>ph</sub>,H<sub>ph</sub>), 7.67 (s, 1H,H<sub>3</sub>), 7.55 (d, H<sub>8</sub>), 7.37 (pst, 2H,H<sub>ph</sub>), 7.27 (pst,1H,H<sub>ph</sub>), 7.03(Pst,1H,H<sub>7</sub>),6.58(t,1H,H<sub>6</sub>).

RMN <sup>13</sup>C (100 MHz, CDCl<sub>3</sub>) δ(ppm): 145.36 (C<sub>8a</sub>/C<sub>2</sub>), 133.56 (C<sub>ph</sub>), 130.18 (C<sub>5</sub>), 128.53 (2C<sub>ph</sub>), 127.76 (C<sub>ph</sub>), 125.82(2C<sub>ph</sub>),125.47(C<sub>5</sub>),124.50 (C<sub>7</sub>), 117.07 (C<sub>8</sub>), 112.15 (C<sub>6</sub>), 108.04 (C<sub>3</sub>).

P5

The 2-(m-methoxyphenyl) imidazo[1,2-a]pyrimidine was provided by *Benchat* and co-workers, by the following method [34]. The synthetic strategy involves condensation of 2-amino pyrimidine with (37.64 g, 0.4 mole) bromoacetometamethoxyphenone (48.75 g, 0.25 mole) in boiling ethanol for five hours, after cooling the solution the mixture has neutralized at 0° C with Na<sub>2</sub>CO<sub>2</sub>, the products are extracted with dichloromethane. The organic layer is dried over sodium sulphate and the dichloromethane is removed under reduced pressure. The crude products are purified on a silica gel column and a colourless solid is obtained. The 2-(m-methoxyphenyl) imidazo[1,2-a]pyrimidine compound is obtained with a good yield 65%.

White powder, M. p. = 226-229 °C;

RMN <sup>1</sup>H (300.134 MHz, CDCl<sub>3</sub>) δ(ppm): 8.50 (dd, 1H, H<sub>5</sub>), 8.40(dd, 1H,H<sub>7</sub>), 8.25 (m,2H, H<sub>ph</sub>), 7.80 (s, 1H,H<sub>3</sub>), 7.27 (pst,1H,H<sub>ph</sub>), 7.4(m,1H,H<sub>ph</sub>),6.80(m,1H,H<sub>6</sub>),3.30(s,3H,OCH<sub>3</sub>).

### 2.3. Measurements

#### 2.3.1. Weight loss measurements

Gravimetric measurements were carried out in a double-walled glass cell equipped with a thermostat cooling condenser. The solution volume was 50 mL. The steel specimens used had a rectangular form (1cm × 1cm × 0.05cm). The immersion time for the weight loss was 6 h at 308 K.

#### 2.3.2. Electrochemical measurements

##### *Electrochemical cell*

The electrolysis cell was Pyrex of cylinder closed by cap containing five openings. Three of them were used for the electrodes. The working electrode was C38 steel with the surface area of 1 cm<sup>2</sup>. Before each experiment, the electrode was polished using emery paper until 1200 grade. After this, the electrode was cleaned ultrasonically with distilled water. A saturated calomel electrode (SCE) was used as a reference. All potentials were given with reference to this electrode. The counter electrode was a platinum plate of surface area of 1 cm<sup>2</sup>. The aggressive medium used here is 1M HCl solution was prepared with concentrated HCl and distilled water. The organic compounds tested are imidazo-

pyridine derivatives. Its molecule formula is shown in Fig. 1. The concentration range of this compound was  $10^{-3}$  to  $10^{-6}$  M.

#### *Polarisation measurements*

The working electrode was immersed in test solution during 30 minutes until a steady state open circuit potential ( $E_{ocp}$ ) was obtained. The polarization curve was recorded by polarization from -800 mV to 500 mV under potentiodynamic conditions corresponding to 1 mV/s (sweep rate) and under air atmosphere, at frequencies between 100 kHz and 100 mHz was superimposed on the rest potential. The potentiodynamic measurements were carried out using Tacussel Radiometer PGZ 301, which was controlled by a personal computer.

### 3. RESULTS AND DISCUSSION

#### 3.1. Gravimetric measurements

##### 3.1.1. Effect of concentration

In the gravimetric experiment, a previously weighed metal (C38 steel) coupon was completely immersed in 50 mL without and with different concentrations of P1 and P5 in an open beaker. The beaker was inserted into a water bath maintained at 308 K. From the weight loss results, the inhibition efficiency (% IE) of the inhibitor and degree of surface coverage ( $\Theta$ ) were calculated using equations 1 and 2 [34];

$$\%IE = \left(1 - \frac{W_1}{W_2}\right) \times 100 \quad (1)$$

$$\Theta = 1 - \frac{W_1}{W_2} \quad (2)$$

Where  $W_1$  and  $W_2$  are the weight losses for steel in the presence and absence of the inhibitor in HCl solution and  $\Theta$  is the degree of surface coverage of the inhibitor.

The values of percentage inhibition efficiency and corrosion rate obtained from weight loss method at different concentrations at 308K are summarized in Table 1. Examination of values indicates clearly a net decrease in the corrosion rate of steel in the presence of our inhibitors. In other words, their inhibition efficiency increased to reach the higher value of 98.8% for P5 and 95.3% for P1 at  $10^{-3}$ M. This may be interpreted by the presence of seven double bonds near three nitrogen atoms and one oxygen atom in the structure of P5 and two nitrogen atoms in the structure of P1, and P5 inhibits further corrosion of C38 steel as it contains more heteroatoms as P1.

The presence of this kind of cyclic rings and the heteroatoms facilitates the adsorption process. The variation in the degree of surface coverage and corrosion rate in the presence of these two compounds may be interpreted by the addition of a second N atom in pyrimidine aromatic cycle: the

efficiency passed from 95.3% to 98.8 % at P1 and P5 at  $10^{-3}$ M, respectively as shown in Fig. (2, 3) and Table 1.

**Table 1.** Gravimetric results of C38 steel in 1M HCl at different concentration of each inhibitor at 6h and 308 K.

Inhibitors	Conc (M)	$W_{\text{corr}}$ (mg/cm <sup>2</sup> h)	$E_w$ (%)	$\Theta$
Blank	1	1.14	-----	-----
P1	$1 \times 10^{-6}$	0.591	48.1	0.481
	$1 \times 10^{-5}$	0.403	64.6	0.646
	$5 \times 10^{-5}$	0.266	76.7	0.767
	$1 \times 10^{-4}$	0.217	81.2	0.812
	$5 \times 10^{-4}$	0.086	92.5	0.925
	$1 \times 10^{-3}$	0.053	95.3	0.953
P5	$1 \times 10^{-6}$	0,559	51.0	0.510
	$1 \times 10^{-5}$	0.310	72.8	0.728
	$5 \times 10^{-5}$	0.223	80.4	0.804
	$1 \times 10^{-4}$	0.150	86.8	0.868
	$5 \times 10^{-4}$	0,048	95.7	0.957
	$1 \times 10^{-3}$	0.014	98.8	0.988

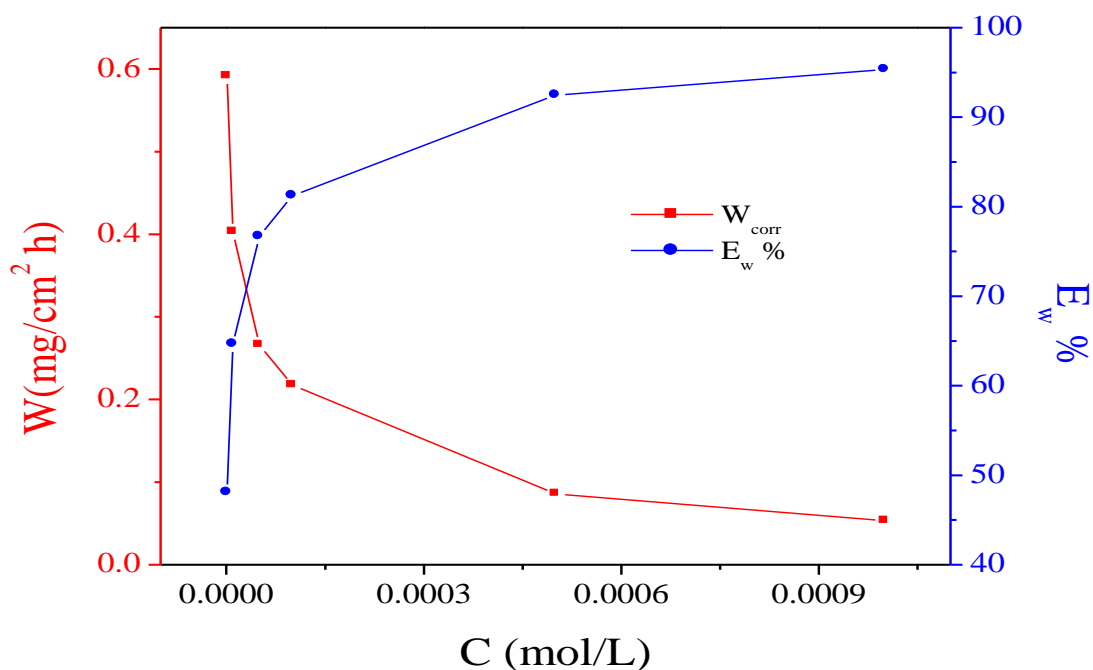


**Figure 2.** Variation of inhibition efficiency and corrosion rate in 1M HCl on C38 steel surface without and with different concentrations of P1.

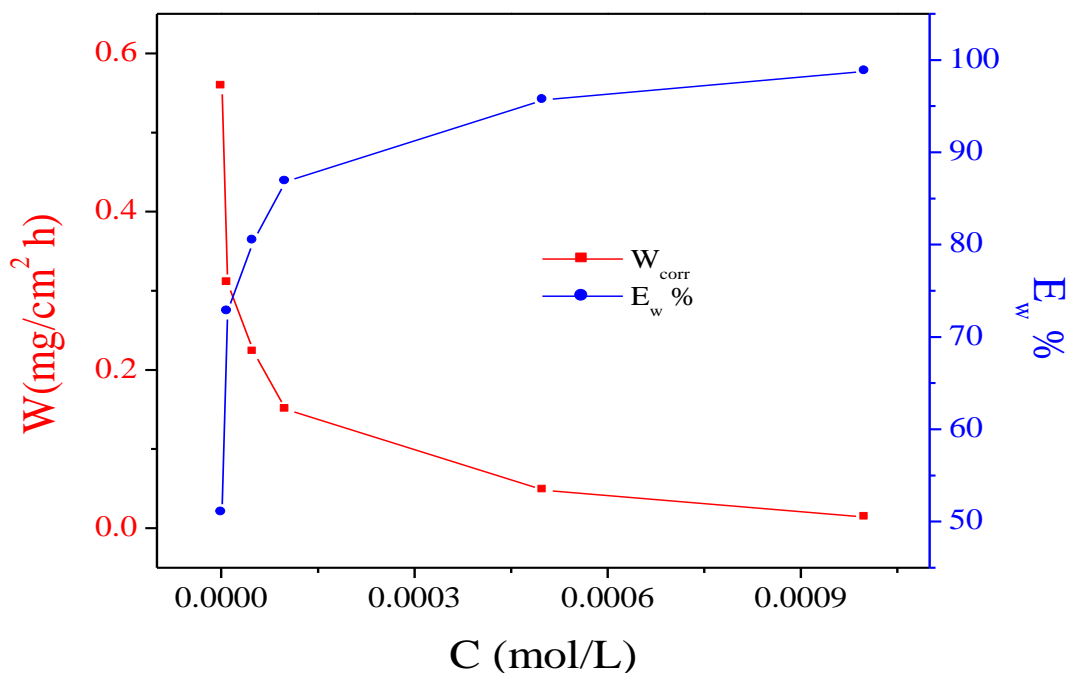


**Figure 3.** Variation of inhibition efficiency and corrosion rate in 1M HCl on C38 steel surface without and with different concentrations of P5.

3.1.2. Effect of temperature and thermodynamic activation parameters

To elucidate the mechanism of inhibition and to determine the thermodynamic parameters of the corrosion process weight loss measurements were performed at 308, 313, 323, 333 and 343K in absence and presence of inhibitors at optimum concentration. The corresponding data are shown in Table 2.

**Table 2.** Various corrosion parameters for steel in 1M HCl in absence and presence of optimum concentration of P1 and P5 at different temperatures at 1h.

Temp (K)	Inhibitors	C <sub>R</sub> (mg/cm <sup>2</sup> h)	E <sub>w</sub> (%)	Θ
308	Blank	1.142	-----	-----
	P1	0.053	95.32	0.9532
	P5	0.014	98.77	0.9877
313	Blank	1.580	-----	-----
	P1	0.094	94.03	0.9403
	P5	0.029	98.16	0.9816
323	Blank	3.027	-----	-----
	P1	0.320	89.47	0.8947
	P5	0.120	96.03	0.9603
333	Blank	5.150	-----	-----
	P1	2.543	82.20	0.8220
	P5	0.402	92.20	0.9220
343	Blank	9.000	-----	-----
	P1	2.543	71.74	0.7174
	P5	1.461	83.77	0.8377

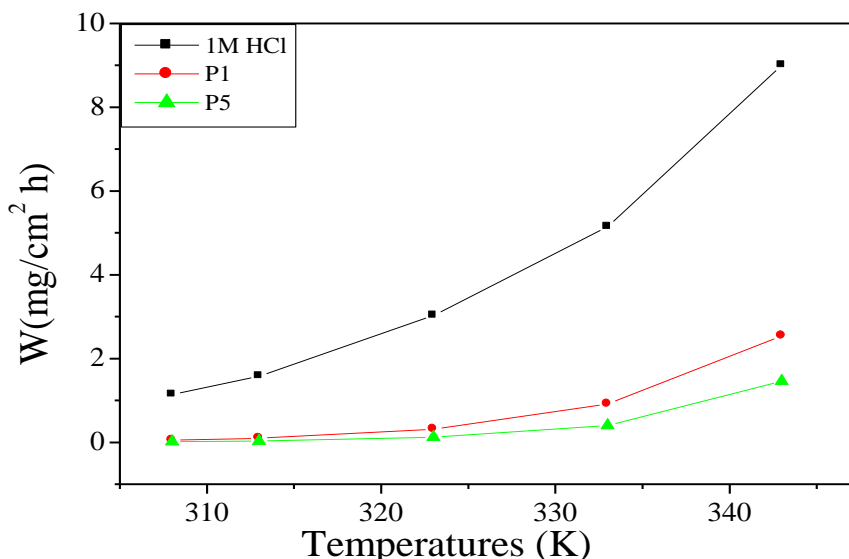


**Figure 4.** Variation of corrosion rate in 1M HCl on steel surface without and with of optimum concentration of P1 and P5 at different temperatures.

Inspection of Table 2 showed that corrosion rate increased with increasing temperature both in uninhibited and inhibited solutions while the inhibition efficiency of P1 and P5 products decreased with temperature. A decrease in inhibition efficiencies with the increase temperature in presence of our compounds might be due to weakening of physical adsorption.

In order to calculate activation parameters for the corrosion process, Arrhenius Eq. (3) and transition state Eq. (4) were used [35]:

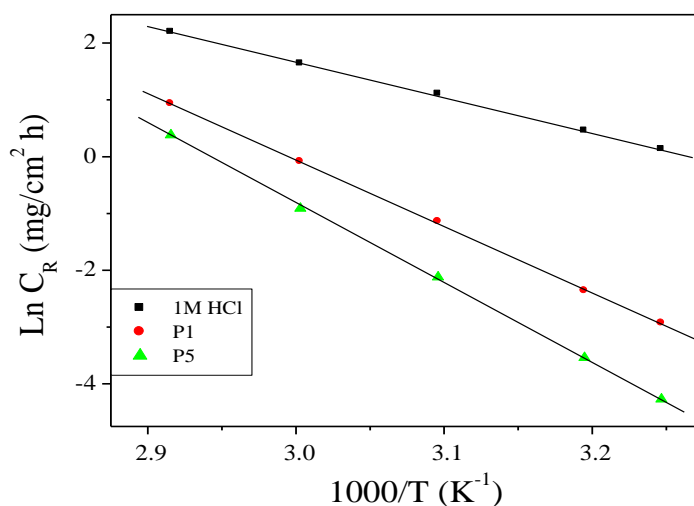
$$C_R = A \exp\left(\frac{-E_a}{RT}\right) \tag{3}$$

$$C_R = \frac{RT}{Nh} \exp\left(\frac{\Delta S_a^\circ}{R}\right) \exp\left(-\frac{\Delta H_a^\circ}{RT}\right) \tag{4}$$

Where  $C_R$  is the corrosion rate,  $R$  the gas constant,  $T$  the absolute temperature,  $A$  the pre-exponential factor,  $h$  the Plank's constant and  $N$  is Avogrado's number,  $E_a$  the activation energy for corrosion process,  $\Delta H_a^\circ$  the enthalpy of activation and  $\Delta S_a^\circ$  the entropy of activation.

The apparent activation energy ( $E_a$ ) at optimum concentration of P1 and P5 were determined by linear regression between  $\ln C_R$  and  $1/T$  (Fig. 5) and the result is shown in Table 3. The linear regression coefficient was close to 1, indicating that the steel corrosion in hydrochloric acid can be elucidated using the kinetic model. Inspection of Table 3 showed that the value of  $E_a$  determined in 1M HCl containing our compounds is higher (115.95KJ mol<sup>-1</sup> for P5 and 97.38 kJ mol<sup>-1</sup> for P1) than that for uninhibited solution (51.64 kJ mol<sup>-1</sup>). The increase in the apparent activation energy may be interpreted as physical adsorption that occurs in the first stage [36]. Szauer and Brand explained that the increase in activation energy can be attributed to an appreciable decrease in the adsorption of the

inhibitor on the steel surface with increase in temperature. As adsorption decreases more desorption of inhibitor molecules occurs because these two opposite processes are in equilibrium. Due to more desorption of inhibitor molecules at higher temperatures the greater surface area of steel comes in contact with aggressive environment, resulting increased corrosion rates with increase in temperature [37].



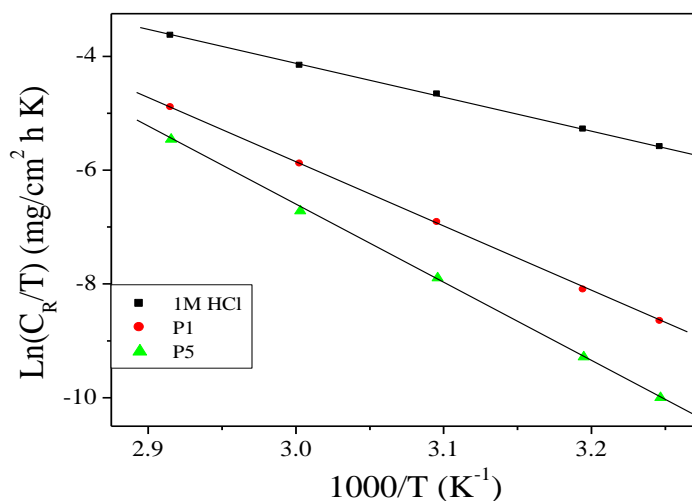
**Figure 5.** Arrhenius plots of Ln C<sub>R</sub> vs. 1/T for steel in 1M HCl in the absence and the presence of P1 and P5 at optimum concentration.

Fig. 6 showed a plot of Ln (C<sub>R</sub>/T) versus 1/T. The straight lines are obtained with a slope ( $\Delta H_a^\circ / R$ ) and an intercept of ( $\ln R/Nh + \Delta S_a^\circ / R$ ) from which the values of the values of  $\Delta H_a^\circ$  and  $\Delta S_a^\circ$  are calculated and are given in Table 3. Inspection of these data revealed that the thermodynamic parameters ( $\Delta H_a^\circ$  and  $\Delta S_a^\circ$ ) for dissolution reaction of steel in 1M HCl in the presence of inhibitors is higher (113.25 kJ/mol for P5 and 94.68 kJ/mol for P1) than that of in the absence of inhibitors (48.95 kJ/mol). The positive sign of  $\Delta H_a^\circ$  reflect the endothermic nature of the steel dissolution process suggesting that the dissolution of steel is slow [38] in the presence of inhibitor.

**Table 3.** Activation parameters for the steel dissolution in 1M HCl in the absence and the presence of P1 and P5 at optimum concentration.

Inhibitor	A (mg/cm <sup>2</sup> h)	Linear regression coefficient (r)	E <sub>a</sub> (kJ/mol)	ΔH <sub>a</sub> <sup>°</sup> (kJ/mol)	ΔS <sub>a</sub> <sup>°</sup> (J/mol.K)
Blank	6,6071×10 <sup>8</sup>	0,99977	51.64	48.95	-85.09
P1	1.7330×10 <sup>15</sup>	0,99991	97.38	94.68	37.78
P5	6.5277×10 <sup>15</sup>	0,99985	115.95	113.25	87.10

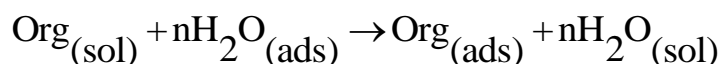
The large negative value of  $\Delta S_a^\circ$  for C38 steel in 1M HCl implies that the activated complex is the rate-determining step, rather than the dissociation step. In the presence of the inhibitors, the value of  $\Delta S_a^\circ$  increases and is generally interpreted as an increase in disorder as the reactants are converted to the activated complexes [18]. The positive values of  $\Delta S_a^\circ$  reflect the fact that the adsorption process is accompanied by an increase in entropy, which is the driving force for the adsorption of the inhibitor onto the steel surface.



**Figure 6.** Arrhenius plots of  $\text{Ln}(C_R/T)$  vs.  $1/T$  for steel in 1M HCl in the absence and the presence of P1 and P5 at optimum concentration.

### 3.1.3. Adsorption isotherm and thermodynamic parameters

It is well recognised that the first step in inhibition of metallic corrosion is the adsorption of organic inhibitor molecules at the metal/solution interface and that the adsorption depends on the molecule's chemical composition, the temperature and the electrochemical potential at the metal/solution interface. In fact, the solvent  $\text{H}_2\text{O}$  molecules could also adsorb at metal/solution interface. So the adsorption of organic inhibitor molecules from the aqueous solution can be regarded as a quasi-substitution process between the organic compounds in the aqueous phase  $[\text{Org}_{(\text{sol})}]$  and water molecules at the electrode surface  $[\text{H}_2\text{O}_{(\text{ads})}]$  [39].



Where (n) is the size ratio, that is, the number of water molecules replaced by one organic inhibitor. Basic information on the interaction between the inhibitor and the steel surface can be provided by the adsorption isotherm. In order to obtain the isotherm, the linear relation between degree of surface coverage ( $\Theta$ ) values ( $\Theta = E\%/100$ ; Table 1) and inhibitor concentration ( $C_{\text{inh}}$ ) must be found. Attempts were made to fit the  $\Theta$  values to various isotherms including Langmuir, Temkin,

Frumkin and Flory–Huggins. By far the best fit is obtained with the Langmuir isotherm. This model has also been used for other inhibitor systems [40, 41]. According to this isotherm,  $\Theta$  is related to  $C_{inh}$  by:

$$\frac{C_{inh}}{\Theta} = \frac{1}{K_{ads}} + C_{inh} \tag{5}$$

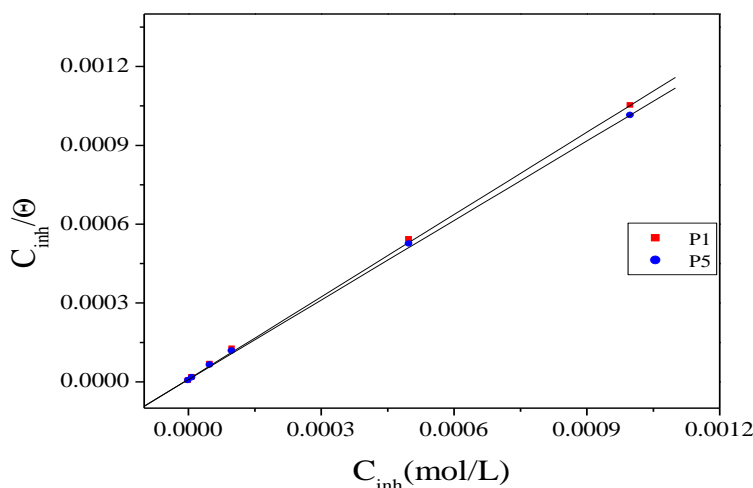
Where  $K_{ads}$  denotes the equilibrium constant for the adsorption process.

Fig. 7 shows the plots of  $C_{inh}/\Theta$  versus  $C_{inh}$  and the expected linear relationship is obtained for all compounds. The strong correlations ( $R^2 = 0.99984$  for the compound P1 and  $R^2 = 0.99985$  for P5) confirm the validity of this approach.

The values of  $K_{ads}$  obtained from the Langmuir adsorption isotherm are listed in Table 4, together with the values of the Gibbs free energy of adsorption  $\Delta G_{ads}^\circ$  calculated from the equation:

$$\Delta G_{ads}^\circ = -RTL \ln(55.5K_{ads}) \tag{6}$$

Where R is the universal gas constant, T the thermodynamic temperature and the value of 55.5 is the concentration of water in the solution [42].



**Figure 7.** Langmuir adsorption of P1 and P5 on the steel surface in HCl solution

The value  $K_{ads}$  calculated from the reciprocal of intercept of isotherm line is indicating in the Table 4. The high value of the adsorption equilibrium constant reflects the high adsorption ability of this inhibitor on C38 steel surface.

**Table 4.** Thermodynamic parameters for the adsorption of P1 and P5 in 1M HCl on the C38 steel at 308K

Inhibitor	Slope	$K_{ads} (M^{-1})$	$R^2$	$\Delta G_{ads}^\circ (kJ/mol)$
P1	1.04	97442.14	0.99984	-39.70
P5	1.01	115628.30	0.99985	-40.14

From Eq. (6),  $\Delta G_{ads}^\circ$  was calculated as  $-39.70 \text{ kJ mol}^{-1}$  for P1 and  $-40.14 \text{ kJ mol}^{-1}$  for P5. The negative value of standard free energy of adsorption indicates spontaneous adsorption of our molecules on C38 steel surface and also the strong interaction between inhibitor molecules and the metal surface [43, 44]. Generally, the standard free energy values of  $-20 \text{ kJ mol}^{-1}$  or less negative are associated with an electrostatic interaction between charged molecules and charged metal surface (physical adsorption); those of  $-40 \text{ kJ mol}^{-1}$  or more negative involves charge sharing or transfer from the inhibitor molecules to the metal surface to form a co-ordinate covalent bond (chemical adsorption) [45, 46]. The value of  $\Delta G_{ads}^\circ$  in our measurement is  $-39.70 \text{ kJ mol}^{-1}$  for P1 and  $-40.14 \text{ kJ mol}^{-1}$  for P5 (in Table 4), it is suggested that the adsorption of this P1 and P5 involves two types of interactions: chemisorption and physisorption [47].

3.2. Polarization curves

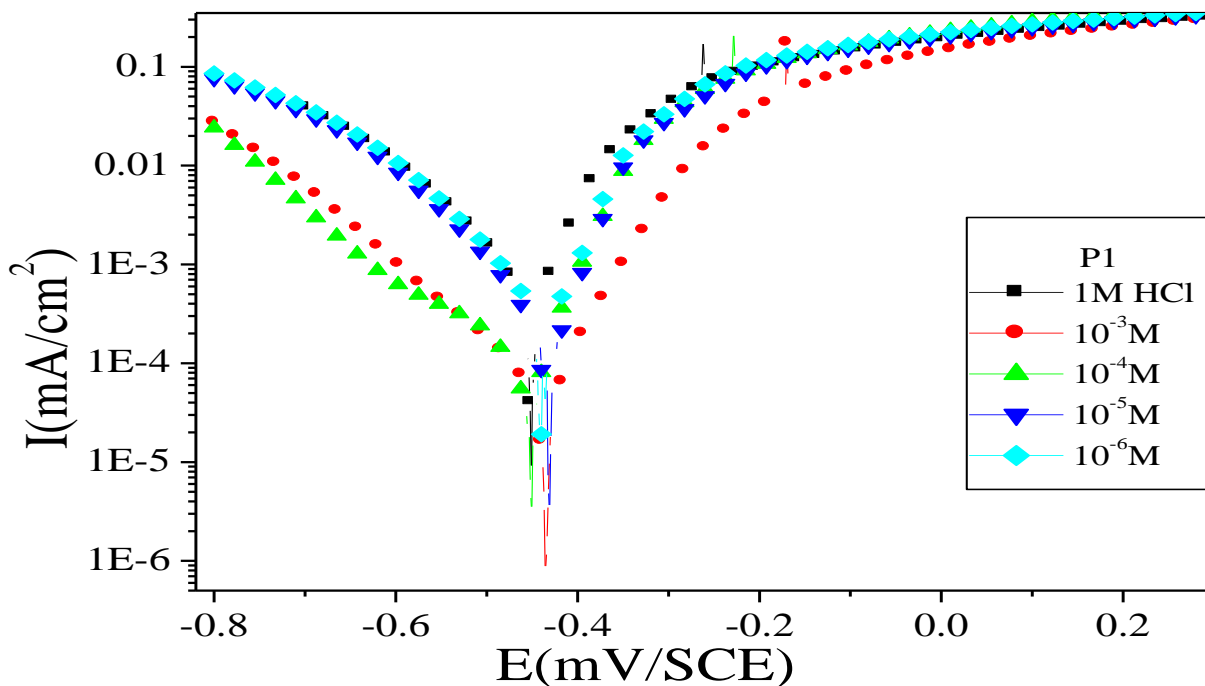


**Figure 8.** Polarization curves of mild steel in 1M HCl containing different concentrations of P1

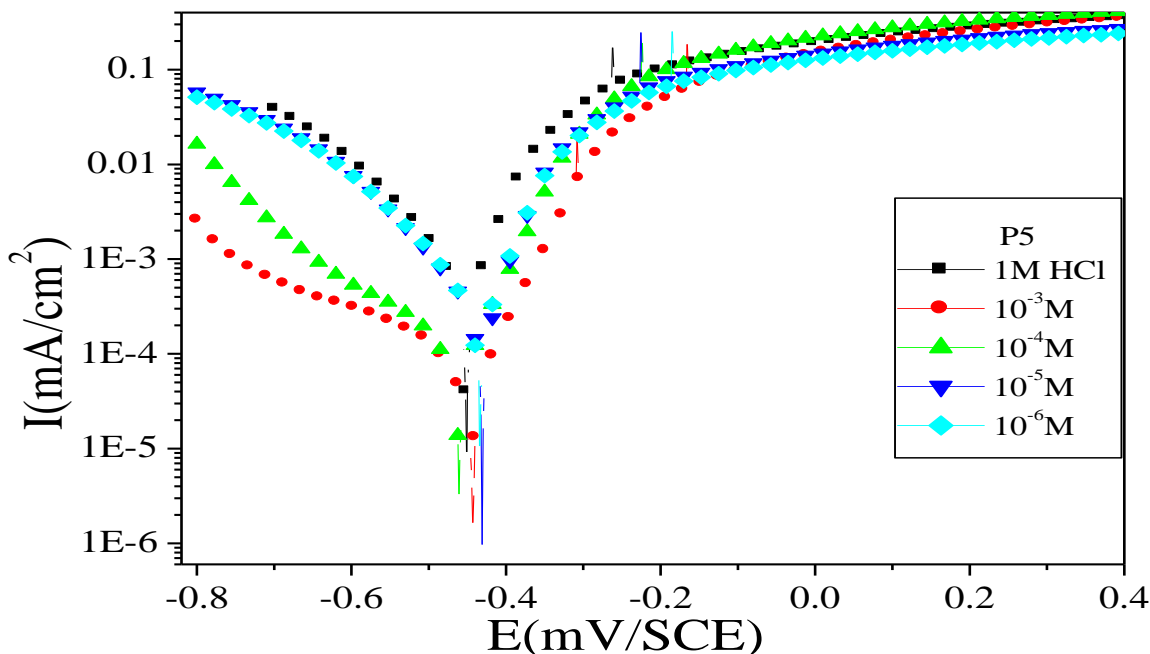


**Figure 9.** Polarization curves of C38 steel in 1M HCl containing different concentrations of P5.

Figs. 8, 9 show typical Tafel curves obtained for C38 steel in 1M HCl with and without the compounds studied. The values of associated electrochemical parameters, i.e., corrosion potential ( $E_{corr}$ ), corrosion current density ( $I_{corr}$ ), cathodic Tafel slopes ( $\beta_c$ ) and percentage inhibition efficiency (IE (%)) values were calculated from polarization curves and listed in Table 5. The inhibition efficiency IE (%) was calculated from polarization measurements according to the relation given below:

$$E_I(\%) = \left( \frac{I_{corr} - I'_{corr}}{I_{corr}} \right) \times 100 \tag{7}$$

Where  $I_{corr}$  and  $I'_{corr}$  are uninhibited and inhibited corrosion current densities, respectively. They are determined by extrapolation of Tafel lines to the respective corrosion potentials.

It is seen that the addition of various inhibitors affects the polarization curves and consequently decreases  $I_{corr}$  significantly, due to increase in the blocked fraction of electrode surface by adsorption.

The data in Table 5 show that increasing compound concentrations slightly shifts the values of corrosion potential ( $E_{corr}$ ) in a cathodic direction indicating that they act as mixed-type inhibitors. The cathodic Tafel slope ( $\beta_c$ ) shows a change with the addition of P1 and P5, which suggests that the inhibiting action occurred by simple blocking of the available cathodic sites on the metal surface, which led to a decrease in the exposed area necessary for hydrogen evolution and lowered the dissolution rate with increasing inhibitor concentration. In the anodic domain, the presence of P1 and P5 decreases anodic current density, the highest effect is observed with there products increase of the over voltage near the corrosion potential. For an over voltage higher than -200 mV/SCE, the presence

of these inhibitors does not change the current density-potential characteristics. This fact means that the inhibition mode of our products depends upon electrode potential. This means that the inhibition mode of inhibitor depends on the electrode potential.

Table 5 clearly indicates a decrease in the corrosion rate (CR) in the presence of P1 and P5. This effect is hugely marked at higher concentrations of inhibitors. The inhibitive action is more explicit using  $E_I\%$  data which increases with inhibitor concentration to reach 92.2% for P1 and 95.7% for P5 at  $10^{-3}M$ . The two inhibitors studied inhibited the corrosion of steel in 1 M HCl, but the inhibitor P5 was found to exhibit the best inhibitory action.

The high values of  $E_I$  observed in molecules P1 and P5 may be explained by the presence of nitrogen atoms,  $\pi$ -electron of bipyrazole rings, and methyl (electron donor groups by inductive effect). The nitrogen atoms are the major adsorption centers for their interaction with the metal surface [48]. The P5 molecule gives more inhibition efficiency than P1, this enhanced efficiency may be due to the replacement of hydrogen atom in P1 molecule by  $-OCH_3$  group.

**Table 5.** Polarization data of C38 steel in 1M HCl without and with addition of inhibitor at 308 K

Inhibitors	Conc (M)	$-E_{corr}$ (mV/SCE)	$-\beta_c$ (mV/dec)	$I_{corr}$ ( $\mu A/cm^2$ )	$E_I$ (%)
Blank	1	455.2	127.3	815.7	-- ----
P1	$10^{-6}$	444.7	106.1	418.9	48.6
	$10^{-5}$	436.4	103.0	257.7	68.4
	$10^{-4}$	456.3	129.9	124.1	84.8
	$10^{-3}$	440.0	136.3	063.6	<b>92.2</b>
P5	$10^{-6}$	438.2	125.2	392.2	51.9
	$10^{-5}$	433.7	109.1	268.9	67.0
	$10^{-4}$	465.9	208.1	119.4	85.4
	$10^{-3}$	448.3	103.8	034.8	<b>95.7</b>

### 3.3. Electrochemical impedance spectroscopic studies

The corrosion behavior of steel, in 1M HCl solution with and without inhibitors, was also investigated by electrochemical impedance spectroscopy (EIS) measurements at 308 K after 30 min of immersion. Figs. 10, 11 showed impedance behavior of steel corrosion in the form of Nyquist plots. The impedance parameters derived from these plots are given in Table 6. Double layer capacitance values ( $C_{dl}$ ) and charge-transfer resistance values ( $R_{ct}$ ) were obtained from impedance measurements. In the case of the electrochemical impedance spectroscopy,  $E_{R_{ct}}$  (%) is calculated by charge transfer resistance according to the relation:

$$E_{R_{ct}} \% = \frac{R_{ct(inh)} - R_{ct}}{R_{ct(inh)}} \times 100 \quad (8)$$

Where  $R_{ct(inh)}$  and  $R_{ct}$  are the charge transfer resistance in the presence and absence of pyridazine, respectively.

The charge-transfer resistance values ( $R_{ct}$ ) were calculated from the difference in real impedance at lower and higher frequencies as suggested by Tsuru et al. [49]. To obtain the double-layer capacitance ( $C_{dl}$ ), the frequency at which the imaginary component of the impedance is maximum ( $-Z_{imax}$ ) is found and  $C_{dl}$  values were obtained from the equation 9:

$$f(-Z_{imax}) = \frac{1}{2\pi C_{dl} R_{ct}} \tag{9}$$

For Nyquist plots (Fig 10, 11) it is clear that the impedance diagrams contain depressed semicircle with centre under real axis. The size of the semicircle increases with the inhibitor concentration, indicating the charge transfer process as the main controlling factor of the corrosion of C38 steel. It is apparent from the plot that the impedance of the inhibited solution has increased with the increase in the concentration of the inhibitors. The experimental result of EIS measurements for the corrosion of C38 steel in 1M HCl in the absence and presence of inhibitors is given in Table 6. As it can be observed from the table, the charge-transfer resistance values ( $R_{ct}$ ) increased with increase in the concentration of the inhibitor whereas values of the capacitance of the interface ( $C_{dl}$ ) starts decreasing, with increase in inhibitor concentration, which is most probably due to the decrease in local dielectric constant and/or increase in thickness of the electrical double layer. This suggests that the inhibitor acts via adsorption at the metal/solution interface [50] and the decrease in the  $C_{dl}$  values is caused by the gradual replacement of water molecules by the adsorption of the inhibitor molecules on the electrode surface, which decreases the extent of metal dissolution [51]. A decrease in the  $C_{dl}$  values with increase of the concentration of inhibitor is shown in Fig. 12. The inhibiting effectiveness increases with the concentration of the inhibitors to reach a maximum value from 90.8% for P5 and 89.0 % for P1 to  $10^{-3}M$ .

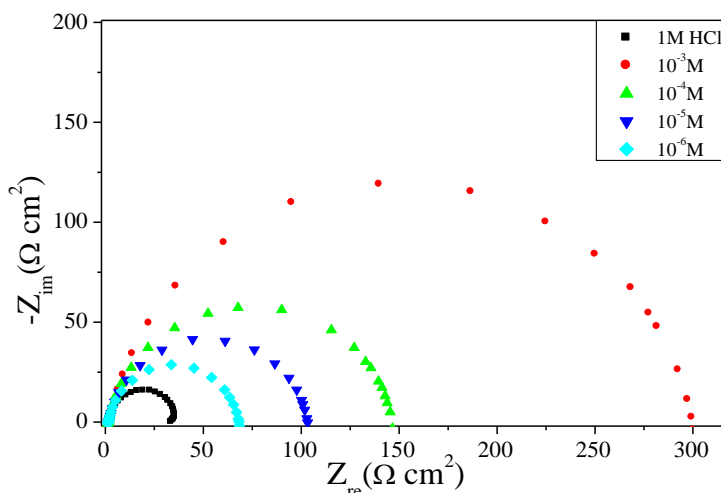


Figure 10. Nyquist diagrams C38 steel in 1M HCl without and with different concentrations of P1.

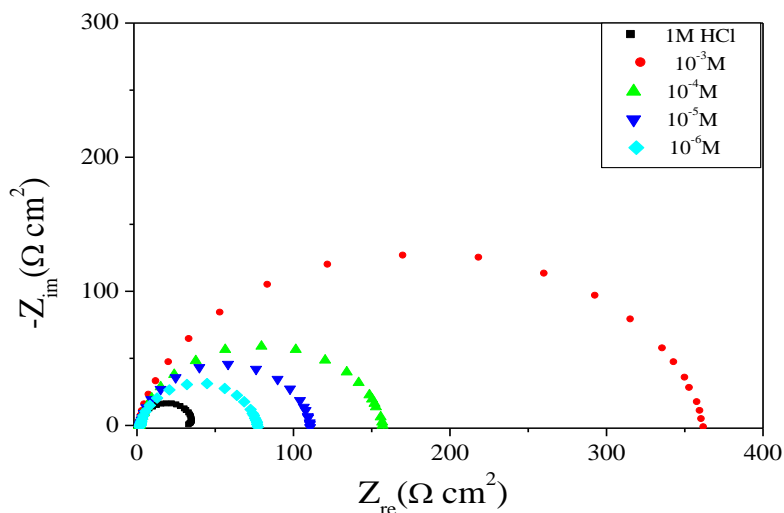
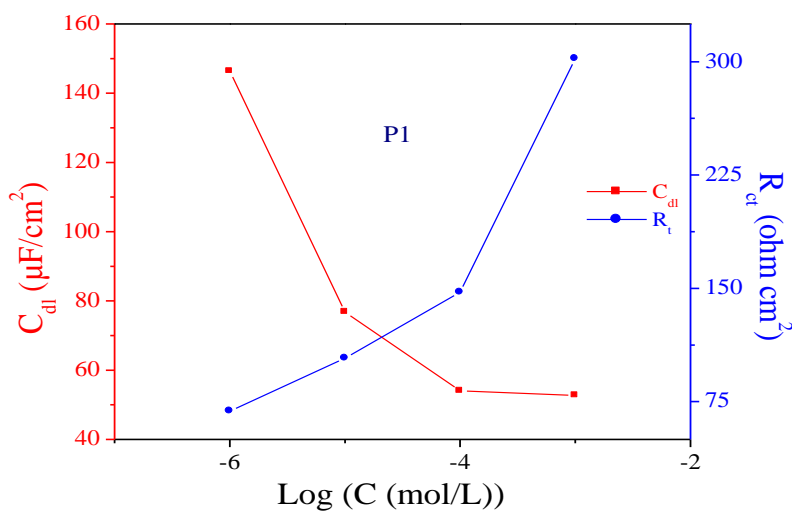
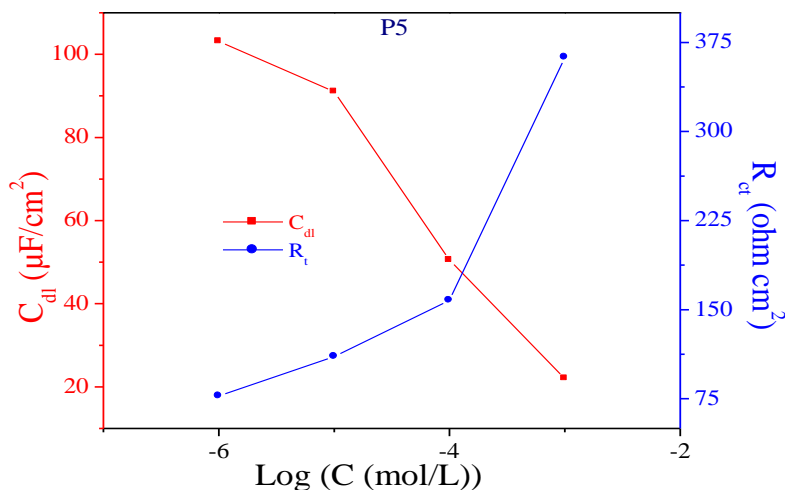


Figure 11. Nyquist diagrams C38 steel in 1M HCl without and with different concentrations of P5.

Table 6. Impedance parameters of C38 steel in 1M HCl containing different concentrations of P1 and P5 compounds.

Inhibitors	Conc (M)	$R_{ct}$ ( $\Omega\text{ cm}^2$ )	$F_{max}$ (Hz)	$C_{dl}$ ( $\mu\text{F cm}^2$ )	$E_{Rct}$ (%)
Blank	1	033.2	50.00	095.8	-----
P <sub>1</sub>	$10^{-6}$	068.8	15.82	146.3	51.7
	$10^{-5}$	103.7	20.00	76.8	67.9
	$10^{-4}$	147.4	20.00	54.0	77.4
	$10^{-3}$	302.0	10.00	52.7	89.0
P <sub>5</sub>	$10^{-6}$	077.2	20.00	103.1	57.0
	$10^{-5}$	110.6	15.82	091.0	69.9
	$10^{-4}$	157.7	20.00	050.5	78.9
	$10^{-3}$	362.6	20.00	022.0	90.8





**Figure 12.** Evolution of transfer resistance and capacitance as function of logarithm of P1 and P5 concentration.

A comparison may be made between inhibition efficiency  $E$  (%) values obtained by different methods (weight loss, polarisation curves and EIS methods). Fig.13 shows a curve that compares the  $E$  (%) values obtained. One can see that whatever the method used, no significant changes are observed in  $E$  (%) values. We can then conclude that there is a good correlation with the three methods used in this investigation at all tested concentrations and that our products are efficient inhibitors of corrosion.

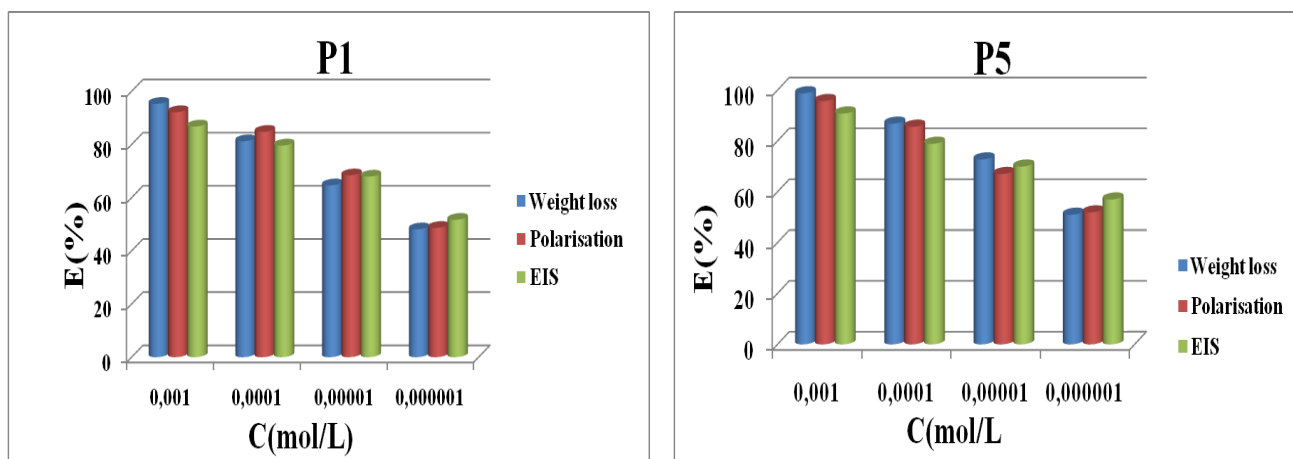


**Figure 13.** Comparison of inhibition efficiency ( $E$  %) values obtained by weight loss, polarisation and EIS methods.

#### 4. CONCLUSION

The main conclusions drawn from this study are:

- P1 and P5 inhibits the corrosion of C38 steel in 1M HCl. The inhibition efficiency depends on the molecular structure.
- P1 and P5 adsorbs according to the Langmuir isotherm model.
- The inhibition efficiency increases with increasing inhibitor concentrations to attain a maximum value of 98.8% for inhibitor P5 and 95.3% for inhibitor P1 at  $10^{-3}$ M.
- The negative values of  $\Delta G_{ads}^{\circ}$  indicate that the adsorption of the inhibitors molecule is a spontaneous process and an adsorption mechanism is typical of chemisorption and physisorption.
- The inhibition efficiency decreased with increasing temperature as a result of the higher dissolution of steel at higher temperature.
- Kinetic and adsorption parameters were evaluated and discussed.
- Polarization study shows that compounds act as mixed-type inhibitors.
- Impedance method indicates that compounds adsorbs on C38 steel surface with increasing charge transfer resistance and decreasing the double-layer capacitance.

#### ACKNOWLEDGEMENTS

Prof S. S. Al-Deyab and Prof B. Hammouti extend their appreciation to the Deanship of Scientific Research at king Saud University for funding the work through the research group project.

#### References

1. M. Batros and N. Hakerman, *J. Electrochem. Soc.* 139 (1992) 3429.
2. F. Bentiss, M. Lagrenee, M. Traisnel, B. Mernari, and H. El Attari, *J. Appl. Electrochem.* 29 (1999) 1073.
3. P. Kutej, J. Vosta, J. Pancir, J. Macak, and N. Hackerman, *J. Electrochem. Soc.* 142 (1995) 829.
4. M. Dahmani, A. Et-Touhami, S.S. Al-Deyab, B. Hammouti and A. Bouyanzer, *Int. J. Electrochem. Sci.* 5 (2010) 1060.
5. J.M. Bastidas, J.L. Polo and E. Cano, *J. Electrochem. Soc.* 30 (2000) 1173.
6. B. Hammouti, A. Zarrouk, S.S. Al-Deyab and I. Warad, *Oriental J. Chem.* 2011, 27, 23.
7. E.E. Foad El Sherbini, *Mater. Chem. Phys.* 60 (1999) 286.
8. W.W. Frenier, F.B. Growcock and V.R. Lopp, *Corrosion.* 44 (1988) 590.
9. M.A. Quraishi and D. Jamal, *Corrosion.* 56 (2000) 156.
10. M. Benabdellah, A. Yahyi, A. Dafali, A. Aouniti, B. Hammouti and A. Ettouhami, *Arab. J. Chem.* 4 (2011) 343.
11. M. Elayyachy, B. Hammouti, A. El Idrissi and A. Aouniti, *Port. Electrochim. Acta.* 29 (2011) 57.
12. J.M. Sykes, *Br. Corros. J.* 25 (1990) 175.
13. P. Chatterjee, M.K. Banerjee and K.P. Mukherjee, *Indian J. Technol.* 29 (1991) 191.
14. JO'M. Bockris, and B. Yang, *J. Electrochem. Soc.* 138 (1991) 2237.
15. A. Zarrouk, I. Warad, B. Hammouti, A. Dafali, S.S. Al-Deyab and N. Benchat, *Int. J. Electrochem. Sci.* 5 (2010) 1516.
16. DA. Vermilyea, in, First International Congress; Metal Corrosion; Butterworths; London; 1962, p 62
17. F. Bentiss, M. Traisnel, N. Chaibi, B. Mernari, H. Vezin and M. Lagrenee, *Corros. Sci.* 44 (2002) 2271.
18. I.El Ouali, B. Hammouti, A. Aouniti, Y. Ramli, M. Azougagh, E.M., Essassi and M. Bouachrine, *J. Mater. Environ. Sci.* 1 (2010) 1.

19. K.F. Khaled, N.S. Abdelshafi, A. El-Maghraby and N. Al-Mobarak, *J. Mater. Environ. Sci.* 2 (2011) 166.
20. J. Uhrea and K. Aramaki, *J. Electrochem. Soc.* 138 (1991) 3245.
21. S. Kertit and B. Hammouti, *Appl. Surf. Sci.* 93 (1996) 59.
22. A. Chetouani, B. Hammouti, A. Aouniti, N. Benchat and T. Benhadda, *Prog. Org. Coat.* 45 (2002) 373.
23. K. Bekkouch, A. Aouniti, B. Hammouti, S. Kertit, *J. Chim. Phys.* 96 (1999) 838.
24. S. Kertit, B. Hammouti, M. Taleb and M.; Brighli, *Bull. Electrochem.* 13 (1997) 241.
25. M. Bouklah, N. Benchat, A. Aouniti, B. Hammouti, M. Benkaddour, M. Lagrenee, H. Vezin and F. Bentiss, *Prog. Org. Coat.* 51 (2004) 118.
26. L. Wang, *Corros. Sci.*, 48 (2006) 608.
27. M. Lagrenee, B. Mernari, N. Chaibi, M. Traisnel, H. Vezin and F. Bentiss, *Corros. Sci.* 43 (2001) 951.
28. S. Rengamani, S. Muralidharan, M. Anbu Kulandainathan and S. Venkatakrishna Iyer, *J. Electrochem. Soc.* 24 (1994) 355.
29. F. Bentiss, F. Gassama, D. Barbry, L. Gengembre, H. Vezin, M. Lagrenee, M. Traisnel, *Appl. Surf. Sci.* 252 (2006) 2684.
30. H. Zarrok, R. Saddik, H. Oudda, B. Hammouti, A. El Midaoui, A. Zarrouk, N. Benchat, M. Ebn Touhami, *Der Pharma Chemica.* 3 (2011) 272.
31. A. Chetouani, B. Hammouti, A. Aouniti, N. Benchat, T. Benhadda, *Prog. Org. Coat.* 45 (2003) 73.
32. M. Bouklah, N. Benchat, A. Aouniti, B. Hammouti, M. Benkaddour, M. Lagrenee, H. Vezin, F. Bentiss, *Prog. Org. Coat.* 51 (2004) 118.
33. Benchat N, Abouricha S, Anafloos A, Mimouni M and Ben-Hadda T, El Bali B, Hakkou A and Hacht B, *Lett Drug Design Discovery*, 2004, 1, 224-229.
34. S. R. Lodha, *Pharmaceutical Reviews.* (2008) 1.
35. J.O'M. Bockris, A.K.N. Reddy, *Modern Electrochemistry, Plenum Press, New York*, 2 (1977) 1267.
36. S. Martinez, I. Stern, *Appl. Surf. Sci.* 199 (2002) 83.
37. T. Szauer, A. Brand, *Electrochim. Acta* 26 (1981) 1219.
38. N.M. Guan, L. Xueming, L. Fei, *Mater. Chem. Phys.* 86 (2004) 59.
39. M. Sahin, S. Bilgic, H. Yilmaz, *Appl. Surf. Sci.*, 195 (2002) 1-7.
40. M. Kissi, M. Bouklah, B. Hammouti, M. Benkaddour, *Appl. Surf. Sci.*, 252 (2006) 4190-4197.
41. E. Machnikova, K. H. Whitmire, N. Hackerman, *Electrochim. Acta.*, 53 (2008) 6024-6032
42. O. Olivares, N. V. Likhanova, B. Gomez, J. Navarrete, M.E. Llanos-Serrano, E. Arce, J. M. Hallen, *Appl. Surf. Sci.*, 252 (2006) 2894-2909.
43. G. Avci, *Mater. Chem. Phys.* 112 (2008) 234.
44. E. Bayol, A.A. Gurten, M. Dursun, K. Kayakirilmaz, *Acta Phys. Chim. Sin.* 24 (2008) 2236.
45. O.K. Abiola, N.C. Oforika, *Mater. Chem. Phys.* 83 (2004) 315.
46. M. Ozcan, R. Solmaz, G. Kardas, I. Dehri, *Colloid Surf. A.* 325 (2008) 57.
47. S. Zhang, Z. Tao, W. Li, B. Hou, *Appl. Surf. Sci.* 255 (2009) 6757.
48. N. Nobe, N. Eldakar, *Corrosion.* 37 (1981) 271.
49. T. Tsuru, S. Haruyama, B. Gijutsu, *J. Jpn. Soc. Corros. Eng.* 27 (1978) 573.
50. K. F. Khaled, *Electrochim. Acta.* 48 (2003) 2493.
51. J. Aljourani, K. Raeissi, and M. A. Golozar, *Corros. Sci.* 51 (2009) 1836.